
Advanced Composite Materials
Publication details, including instructions for authors and subscription information:
http://www.tandfonline.com/loi/tacm20

# Synthesis and Characterization of Al-SiC Nanocomposites Produced by Mechanical Milling and Sintering

S. Kamrani [a] , Z. Razavi Hesabi [b] , R. Riedel [c] & S. M. Seyed Reihani [d]

[a] Department of Material Science and Engineering, Sharif University of Technology, P.O. Box 11365-9466, Azadi Avenue, 14588 Tehran, Iran; Dispersive Solids Group, Darmstadt University of Technology, Petersenstr. 23, D-64287, Germany

[b] Department of Material Science and Engineering, Sharif University of Technology, P.O. Box 11365-9466, Azadi Avenue, 14588 Tehran, Iran

[c] Dispersive Solids Group, Darmstadt University of Technology, Petersenstr. 23, D-64287, Germany

[d] Department of Material Science and Engineering, Sharif University of Technology, P.O. Box 11365-9466, Azadi Avenue, 14588 Tehran, Iran

Version of record first published: 02 Apr 2012.

VSP

*Advanced Composite Materials 20 (2011) 13–27*

ADVANCED COMPOSITE MATERIALS
brill.nl/acm

# Synthesis and Characterization of Al–SiC Nanocomposites Produced by Mechanical Milling and Sintering

**S. Kamrani** [a,b,*], **Z. Razavi Hesabi** [a], **R. Riedel** [b] **and S. M. Seyed Reihani** [a]

[a] Department of Material Science and Engineering, Sharif University of Technology, P.O. Box 11365-9466, Azadi Avenue, 14588 Tehran, Iran

[b] Dispersive Solids Group, Darmstadt University of Technology, Petersenstr. 23, D-64287, Germany

Received 17 September 2008; accepted 28 October 2009



**Abstract**

Aluminum powder and various volume fractions of SiC particles with an average diameter of 50 nm were milled by a high-energy planetary ball mill to produce nanocrystalline Al–SiC nanocomposite powders. Double pressing/sintering process was used to consolidate powders to cylindrical specimens. It was shown that a double cycle of cold pressing and sintering can be utilized to obtain high density Al–SiC nanocomposite parts without using a hot-working step. High resolution scanning electron microscopy (HRSEM), X-ray diffraction (XRD) and laser particle size analyzer (PSA) were used to study the morphological and microstructural evolution of nanocomposite powders and bulk samples. The role of volume fraction of SiC nanoparticles in grain size of both as-milled and as-consolidated aluminum matrix was investigated. It was found that the presence of the higher SiC particles eventuate to slowly decrease in grain size of aluminum matrix powders. However, this trend is strongly noticeable in grain size of consolidated samples. The pinning effects on grain stability by SiC nanoparticles were quantitatively analyzed. It was found that Gladman's model is in close agreement with the experimentally determined grain size of Al–SiC nanocomposites.


**Keywords**

Nanocomposite, mechanical milling, consolidation, grain size, grain stability

## 1. Introduction

In recent years, aluminum matrix composites (AMCs) have received wider acceptance as structural materials in the design of many components. AMCs exhibit a high specific strength and stiffness as well as low coefficient of thermal expansion, which make them attractive for automotive and aerospace industries. It is well known that the characteristics of reinforcement particles significantly influence the mechanical properties of AMCs. For instance, yield and tensile strength increase whereas toughness and ductility decrease with increasing volume frac-

* To whom correspondence should be addressed. E-mail: kamrani@mehr.sharif.ir

 DOI:10.1163/092430410X512676

tion and/or decreasing reinforcement particle size. It has recently been reported that decreasing the reinforcement particle size to nanoscale range is favorable for achieving higher strength. Nanostructured nanocomposites are thus an attractive area for investigation. However, fabrication of these materials is difficult concerning uniform dispersion of nanometric hard particles throughout the metal matrix and retaining the nanostructured matrix after consolidation. Mechanical milling is one of the common methods for production of metal matrix nanocomposites. In this process, a mixture of metal and ceramic powder is usually directly milled to achieve homogeneity of particle distribution throughout the matrix and to form the nanocomposite powder. To obtain bulk composites from mechanically alloyed powders, several consolidation techniques have been employed, such as sintering [1], hot-pressing [2], hot-isostatic pressing [3, 4] and hot extrusion of loose or prepressed powders [5, 6]. It is of practical interest if the nanocomposites are produced by common powder metallurgy route due to its advantages in manufacturing near-net shape parts at lower production cost. To the knowledge of authors, there is little report on fabrication of Al matrix nanocomposites by pressing and sintering route. This relates to the consolidation response of mechanically-alloyed composite powders. Since after MA the particles are work-hardened, generally the compressibility of milled powders is low [7]. The reinforcement particles also bear a part of the applied load during compaction and decrease the green density. Moreover, the solid reinforcement particles retard the sintering response of the metal matrix [8]. In addition, grain growth of the nanocrystalline matrix occurs when a high temperature processing, e.g., sintering, is used.

The aim of the present investigation was to study a process for consolidation of mechanically milled Al nanocomposite powders which eliminates the need for a hot-working step. In addition, the study analyzed the influence of nanometric SiC particles on the stabilization of the Aluminum structure during consolidation at elevated temperatures.

## 2. Methods

Aluminum powder with an average particle size of 41.6 μm and purity >99.7% was supplied by Alfa Aesar (Ward Hill, MA, USA). The shape of the particles was almost spherical with relatively broad particle size distribution, Fig. 1. SiC powder with an average size of 50 nm was supplied by Alfa Aesar. Figure 2 shows the morphology of SiC particles taken by transmission electron microscopy (Philips FEG-C200 TEM).

Composite mixtures comprising different volume fractions (0, 1, 3, 5, 7) of SiC and Al powders were prepared by 20 min blending. To prevent excessive cold welding during milling, 2 wt% stearic acid ($CH_3(CH_2)_{16}COOH$) was used as the process control agent (PCA). Mechanical milling was performed in a planetary ball mill (Pulverisette 5, Fritsch, Germany) using aluminum oxide balls (10 mm) for 16 h. The milling conditions are shown in Table 1. All the handling, mixing and milling

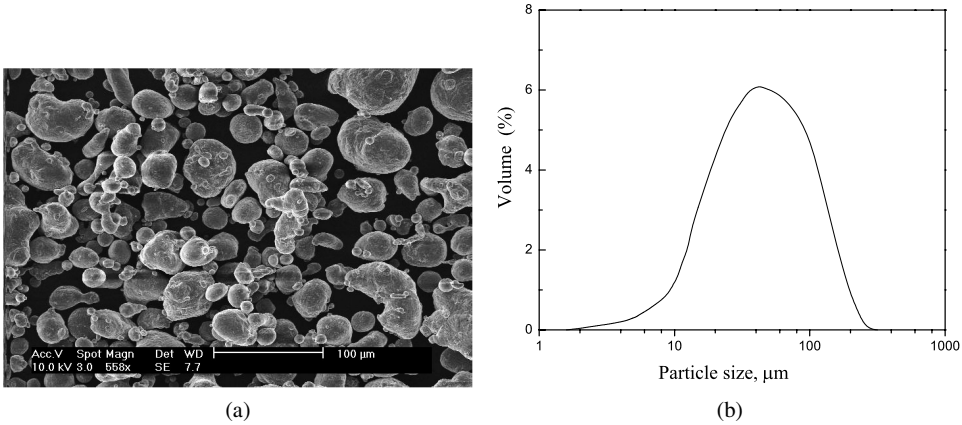


**Figure 1.** Morphology (a) and particle size distribution (b) of aluminum powder.

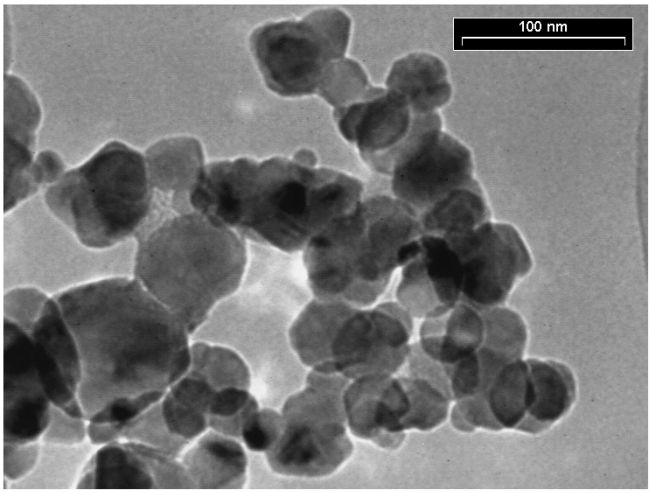


**Figure 2.** TEM micrograph of nanometric SiC particle.

**Table 1.**
Conditions of ball milling process

| | |
|---|---|
| Ratio of ball to powder weight (BPR) | 10:1 |
| Rotational speed (rpm) | 250 |
| Milling time (h) | 16 |
| PCA (wt%) | 2 |

steps were performed under a high purity argon atmosphere. Al powder (without addition of SiC particles) was also processed according to the same procedure for comparison purpose.

**Table 2.**
Consolidation conditions of mechanically milled powders

| Cycle | Step | Pressure (MPa) | Temperature (°C) | Time (min) | Atmosphere |
|---|---|---|---|---|---|
| First | CIP | 200 | – | 10 | Argon |
| | Sintering | – | 640 | 60 | Argon |
| Second | CIP | 500–700* | – | 3 | Argon |
| | Sintering | – | 635 | 30 | Argon |

* Dependent on the SiC content.



The morphology and microstructure of the milled powders were analyzed by using a high resolution scanning electron microscope (PHILIPS XL30 HRSEM). A laser particle size analyzer (Malvern, Worcestershire, UK) was employed to determine the particle size distribution of the powders. The grain size ($d$) and lattice plastic strain ($\varepsilon$) of the metal matrix was determined according to the Willamson–Hall procedure [9] using a Philips X'Pert MPD Diffractometer with Cu $K_\alpha$ radiation.

Double pressing/sintering route was used to consolidate powders to cylindrical specimens. The processing cycles are reported in Table 2. The powders were filled in a polymeric die with a diameter of 20 mm and isostatically cold pressed (CIPed) at 200 MPa for 10 min. The intermediate sintering was performed at 640°C for 60 min. In the second cycle, the specimens were CIPed at constant pressure (500 MPa) and/or a high pressure range from 500 to 700 MPa depending on the SiC content and sintered at 635°C for 30 min. After consolidation, the sintered specimens were annealed at 350°C for 2 h and cooled to ambient temperature in the furnace. All the fabrication steps were carried out under a high purity argon atmosphere.

The density of the compacts was determined by the water displacement (Archimedes) method. Specimens for metallographic were prepared following the common procedure and the microstructure was studied by HRSEM and EDX. An Emcee M1C010 hardness tester was used to measure the hardness of the samples at applied load of 0.5 kgf for 15 s. The hardness values reported were averaged from at least ten indentations on each sample.

## 3. Results

### *3.1. Powder Characteristics*

HRSEM was employed to assess the morphological changes of powder particles after milling. Figure 3 shows the morphology of mechanically milled Al–5%SiC composite powders after 16 h of high energy milling. It is shown that approximately the process reaches a steady state in which welding and fracture are in balance and

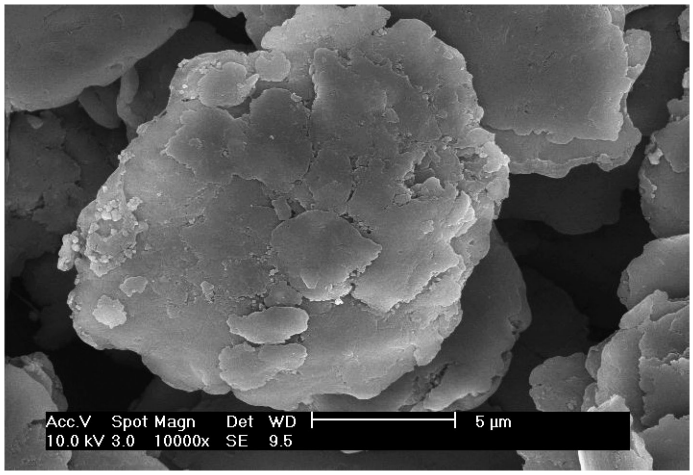


**Figure 3.** Morphology of Al–5%SiC (50 nm) composite powder after 16 h of milling.

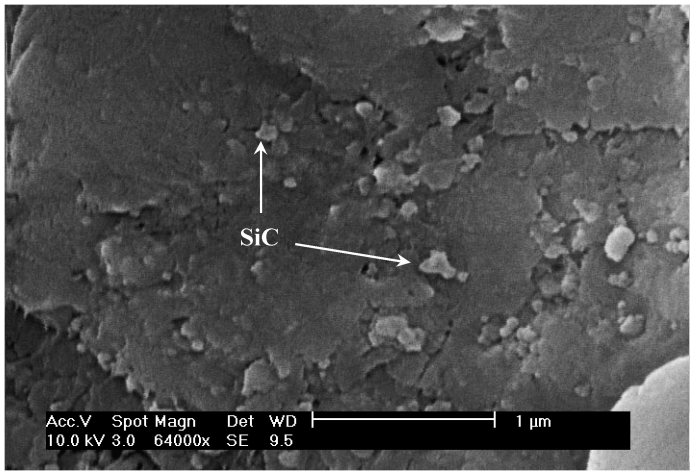


**Figure 4.** Microstructure of Al–5%SiC (50 nm) composite powder after 16 h of milling.

the particle morphology is approximately equiaxed. At this stage, each particle is a composite one produced by mechanical alloying [10], displaying a fine and homogeneous distribution of the nanometric reinforcement through the whole particle, as shown in Fig. 4.

Figure 5 shows the particle size distribution of mechanically milled Al, Al–5%SiC and Al–7%SiC composite powders. As it is seen, all the examined powders have a symmetric log-normal size distribution. An increase in the average particle size of milled Al powder is noticeable and furthermore, the size distribution became broader. By contrast, the size distribution of the composite powders is narrow. The mean particle size of the milled aluminum powders at various volume fractions of SiC particle are shown in Fig. 6. It is found that the higher content of SiC particles results in more reduction of particle size of composite powders.

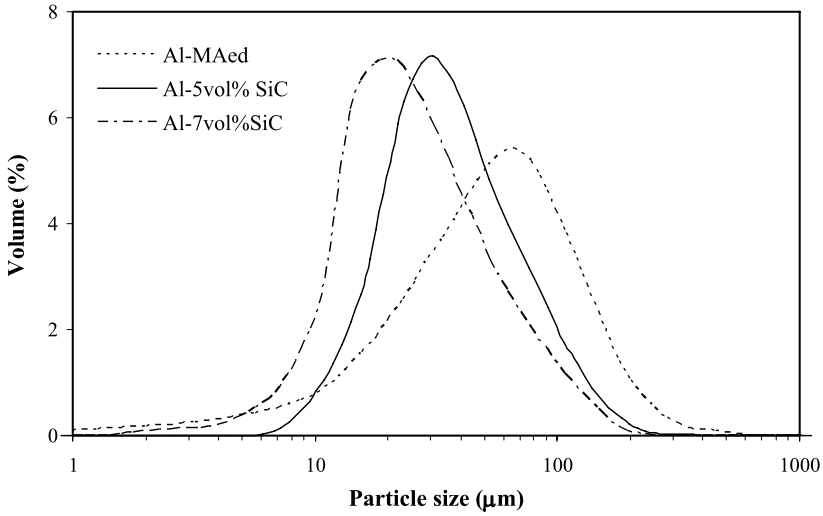


**Figure 5.** Particles size distribution of milled Al and Al–SiC composite powders for 16 h.

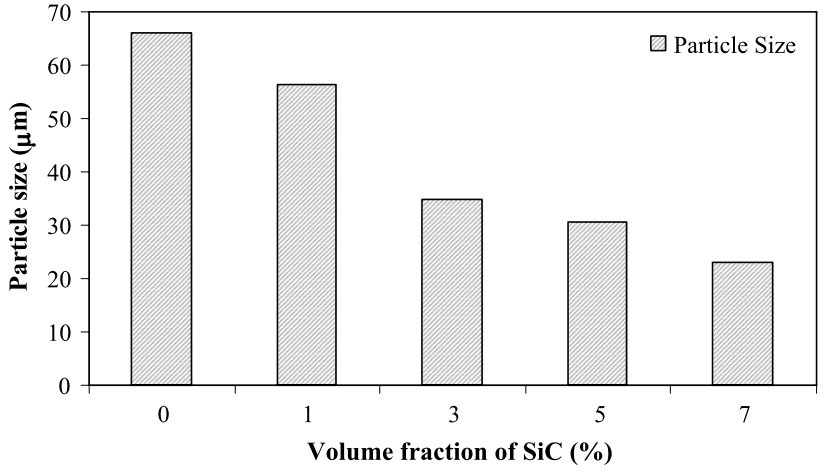


**Figure 6.** Variation of mean particle size of aluminum milled powder *via* SiC nanoparticles content.

In order to evaluate the effect of mechanical milling on the grain refinement of the Al matrix depending on the reinforcement volume fraction, XRD analysis was performed. The analysis of the XRD peaks was performed *via* the Williamson–Hall method according to the following equation [9]:

$$\beta_s \cos\theta = \frac{K\lambda}{d} + 2\varepsilon \sin\theta, \tag{1}$$

where $\beta_s$ is the sample broadening in radians, $\theta$ is the position of peak maximum, $K$ is Scherrer constant ($K = 0.9$ [11]), $\lambda$ is the X-ray wavelength ($\lambda_{Cu} = 0.15405$ nm), $d$ is grain size, and $\varepsilon$ is an approximate upper limit of the lattice

**Table 3.**
Aluminum grain size of milled powder and bulk samples at different volume fraction of SiC particles

| Sample | Grain size (nm) | |
|---|---|---|
| | Powder sample | Bulk sample |
| Al-MAed | 77.76 | 693.22 |
| Al–1%SiC (nm) | 69.32 | 346.61 |
| Al–3%SiC (nm) | 64.12 | 231.07 |
| Al–5%SiC (nm) | 63.02 | 173.30 |
| Al–7%SiC (nm) | 55.45 | 154.05 |



plastic strain. The instrument broadening ($\beta_i$) was removed using the following equation according to Gaussian–Gaussian relationship by silicon powder:

$$\beta_s^2 = \beta_e^2 - \beta_i^2, \tag{2}$$

where $\beta_e$ is the FWHM of the measured XRD peak. The results of XRD analysis of aluminum reinforced with different volume fractions of nanometric SiC are reported in Table 3. It is seen that the grain size of the Al matrix decrease slowly through increase of the SiC volume fraction. Increasing the local plastic deformation of the metal matrix due to more hard particles results in a faster grain refinement as explained elsewhere [12].

### *3.2. Microstructural Aspects and Hardness of Consolidated Materials*

The relative density of the nanocomposites in the first and second cycle of consolidation was plotted against volume fraction of nanometric SiC particles in Fig. 7. As it is seen, after the first cold isostatic pressing, relative density of the samples is about 85–88% of theoretical density. Following the first sintering at 640°C for 1 h, we attain relative densities above 92%, suggesting the formation of fully dense Al–SiC composite material is not achieved. Furthermore, it is seen that the specimens consolidated at second cycle by a constant pressure (500 MPa) and subsequent sintering have higher relative density compare to first consolidation cycle. Nevertheless, fully dense nanocomposite materials are not attained at relatively high SiC content. On the other hand, as it is seen in Fig. 8, all the specimens CIPed in a high pressure range, depending on the SiC content, gain nearly full density ($\geqslant$99.4% TD). This observation indicates that the double pressing/sintering route can be used to obtain high density Al–SiC nanocomposite parts.

HRSEM micrographs of nanometric SiC particles dispersion in the Al matrix of nanocomposite at different volume fractions of reinforcement are shown in Fig. 9. It can be seen that the nanometric SiC particles disperse homogeneously through the bulk samples. EDX analysis of composite specimens shows the presence of aluminum and SiC phases (Fig. 9e).

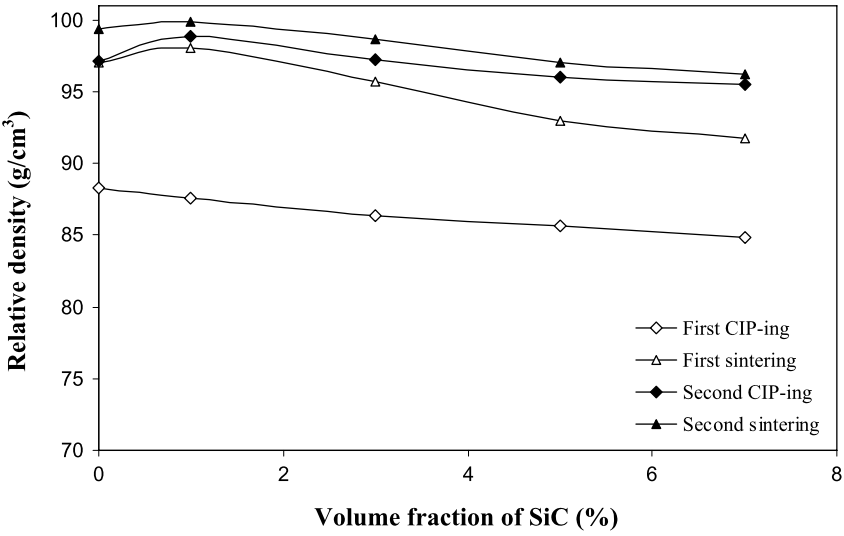


**Figure 7.** Bulk density of Al–SiC nanocomposites at first and second cycle of consolidation (pressure of second cycle = 500 MPa).

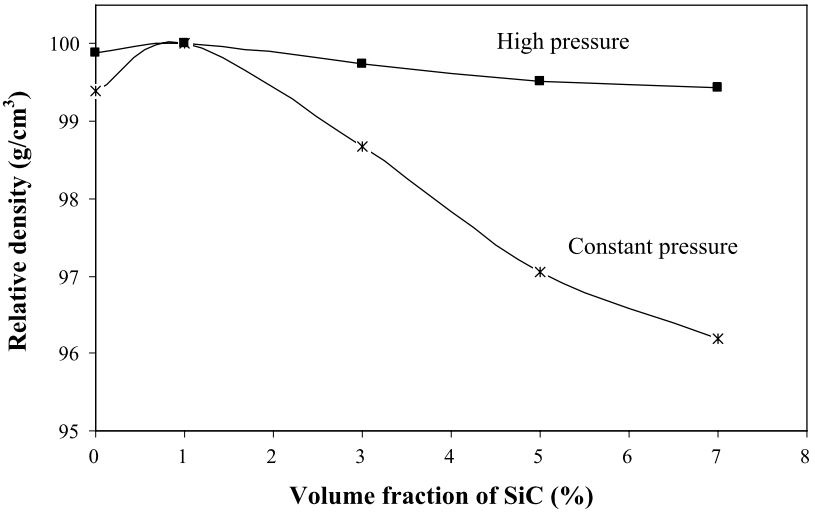


**Figure 8.** Bulk density of Al–SiC nanocomposites at second cycle of consolidation (pressure range from 500 to 700 MPa).

In order to evaluate the grain size of the Al matrix after consolidation process, XRD analysis was performed. The results of XRD analysis of aluminum reinforced with different content of SiC after the consolidation process are reported in Table 3. It can be seen that the nanometric SiC particles have a considerable effect on reduction of aluminum grain size in the consolidated samples.

The hardness measurements of the Al–SiC nancomposites were taken in order to assess the influence of nanometric SiC particle on the mechanical properties. Vick-

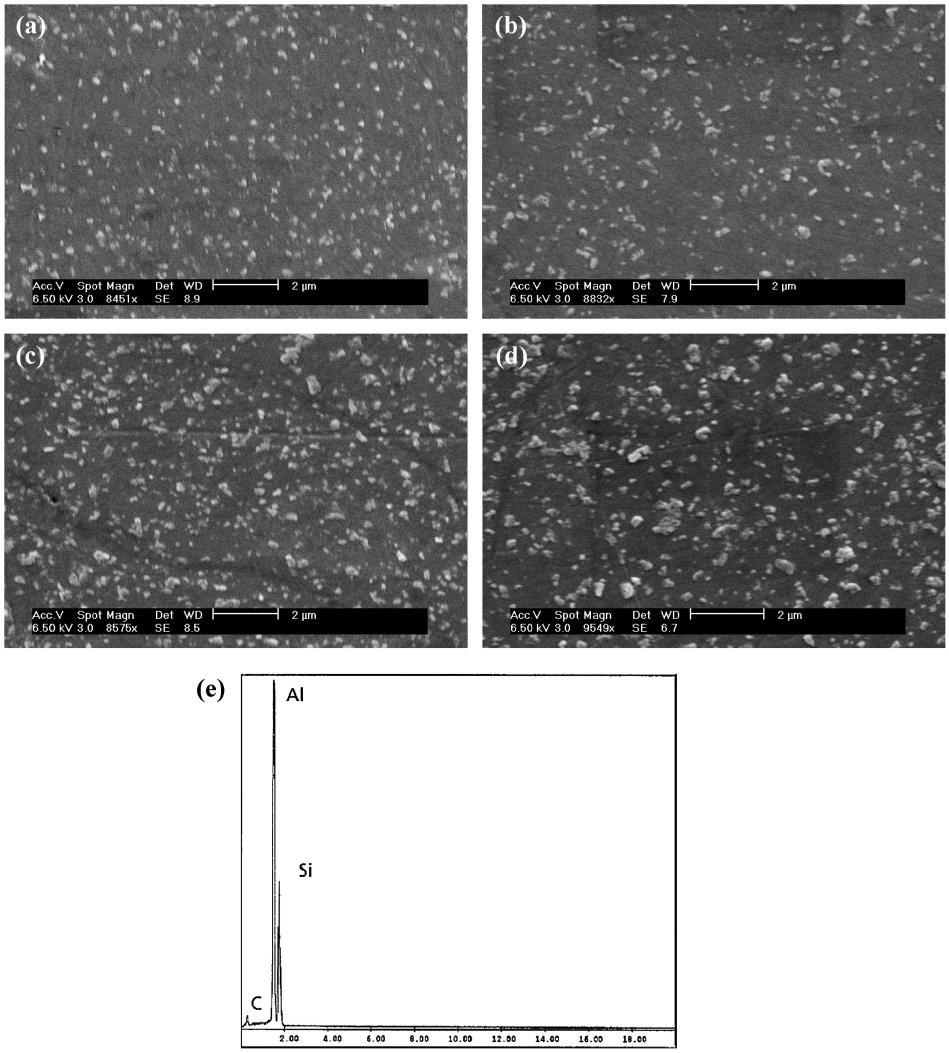


**Figure 9.** Microstructure of consolidated Al–SiC composite powders containing SiC volume fraction (%) of 1 (a), 3 (b), 5 (c), 7 (d) and EDX analysis of the Al–5vol%SiC composite compact (e).

ers hardness as a function of SiC content for the nanocomposite specimens is plotted in Fig. 10. It is observed that the hardness enhances by increasing volume fraction of SiC particles. As, the hardness of aluminum reinforced with 7 vol% nanometric SiC (158 HV) is almost twice the amount of the milled aluminum (unreinforced) specimen (84 HV).

## 4. Discussion

It is shown that densification behavior of the powders depends on the powder characteristics and pressure level [13]. Moreover, work hardening phenomena as

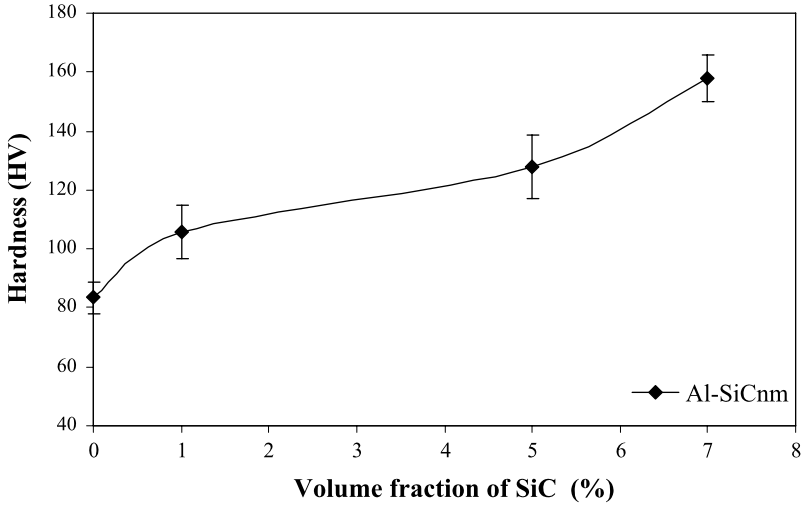


**Figure 10.** Variation of hardness of Al nanocomposite *via* SiC nanoparticles content.

a result of deformation imposed by mechanical milling and hard ceramic particles affect densification behavior of the milled powders [14]. The results of relative density show that second cycle of consolidation has effective role in densification of Al–SiC nanocomposites. However, it is shown at relatively high SiC content, fully dense nanocomposites are not achieved. The analysis of consolidation behavior of mechanically milled aluminum powders under a double pressing/sintering route has been reported by Rodriguez *et al.* [15, 16]. They have shown that the final consolidated compacts have relative densities and mechanical properties comparable to those obtained using well-established hot-working processes. It is revealed that the compressibility of composite powders is lower than that of pure metals and it becomes worse at higher reinforcement volume fractions [17]. The results presented in this work indicated that with increasing the SiC content, finer particles with more refined grain structure is obtained after mechanical alloying. It also enhances the internal strain of aluminum particles [18]. Furthermore, at high volume fractions of hard particles, a connected network of reinforcements forms which supports part or all of the pressure, shielding the soft particles and hindering densification [19]. Thus, it would be difficult to obtain the full density of nanocomposite reinforced by relatively high SiC nanopartcles content. The results reveal that bulk density increases with the increasing of applied pressure in the second pressing/sintering cycle. When the applied pressure increases, the movement of the particles is restricted and the energy applied to the powder compact is spent generally through the process of deformation and friction losses [7, 20]. Therefore, at higher pressures, plastic deformation of ductile powders becomes the predominant densification mechanism. It is worth to notice that the break up of the oxide layer on the surfaces of aluminum powder is easier at enhanced pressures. Therefore, de-

**Table 4.**
Impurity concentration (in wt%) in as-received Al, Al-MAed and Al–5%SiC composite powders

| Powder | As-received Al | Al-MAed | Al–5%SiC |
|---|---|---|---|
| Oxygen | 0.12 | 0.78 | 0.83 |
| Carbon | 0.01 | 0.24 | 2.43 |



velopment of the mechanical bonding between the aluminum particles carries out more straightforward.

The results of the structural study by XRD analysis reveal that in spite of relatively high temperature sintering process, ultra-fine structure of aluminum matrix is practically protected. One may consider the Zener pinning as a contribution to the high grain size stability observed with respect to the presence of nanometric SiC particles distributed homogeneously throughout the aluminum matrix during mechanical milling. It is shown that the particles reduce mobility and energy of grain boundary, hinder the motion of dislocations and finally stabilize the size of nanograins at elevated temperatures [21]. Hence, aluminum matrix with higher content of SiC particles has more potential for pinning of grain boundary and displays lower grain size. It is worth to consider that presence of oxide particles in mechanically milled aluminum matrix. Elemental analysis revealed that 0.12, 0.78 and 0.83 wt% O exists in as received Al, milled Al and Al–5%SiC composite powders, respectively (Table 4). The result indicates oxygen and carbon pick up during processing. The possible sources for the presence of oxide particles are (i) reaction between the aluminum with stearic acid used as PCA [22], (ii) the oxide film covering the surface particles of the gas atomized Al powder, and (iii) abrasion of the balls during milling, probably enhances resistance to grain growth.

Role of fine particles in the control of matrix grain size has been investigated by Zener [23]. Zener proposed that the driving pressure for grain growth due to the curvature of the grain boundary would be counteracted by a pinning (drag) pressure exerted by the particles on the boundary [23, 24]. The zener model predicts a relationship between particle size, volume fraction of particle and matrix grain size (equation (1)):

$$\text{Zener model:} \quad D_{\mathrm{Z}} = \left(\frac{4}{3}\right) \cdot r_{\mathrm{p}} / V_{\mathrm{p}}, \tag{3}$$

where $D_{\mathrm{z}}$ is the predicted grain size of matrix-materials by zener model, $r_{\mathrm{p}}$ is the radius of pinning particles, and $V_{\mathrm{p}}$ is the volume fraction of the particles.

The original derivation of the Zener model did not involve any consideration of the effect of initial grain size distribution on the driving pressure. Gladman [24, 25]

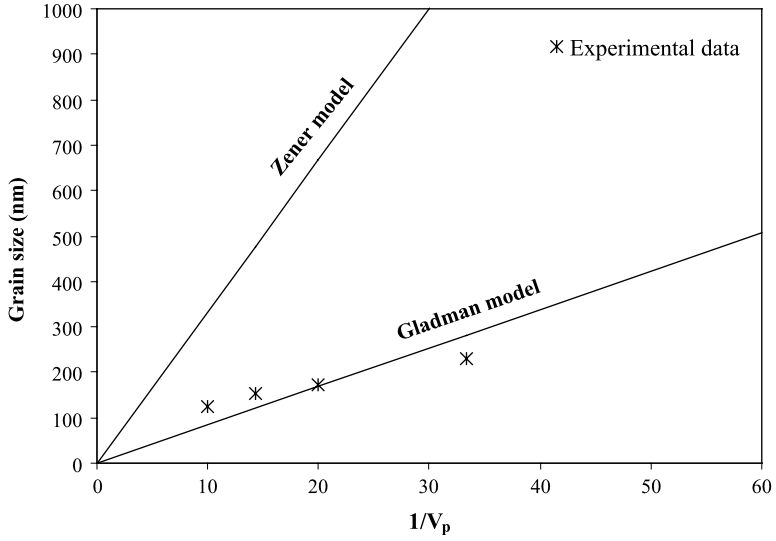


**Figure 11.** Relationship between average grain size of the Al–SiC nanocomposites and $1/V_p$.

analyzed the effect of grain size distribution on the driving pressure (and therefore matrix grain size) and found that:

$$\text{Gladman model:} \quad D_G = \left(\frac{\pi}{3}\right)\left[\frac{3}{2} - \frac{2}{Z}\right] \cdot r_p / V_p, \tag{4}$$

where $D_G$ is the predicted grain size of matrix-materials by Gladman model and $Z$ is the ratio of the diameter of the growing grain to average grain diameter (usually approximated as $Z \approx 1.7$) [26].

The calculated grain sizes of the aluminum matrix reinforced by various volume fractions of SiC particles (50 nm) from zener and gladman models as a function of $1/V_p$ are plotted in Fig. 11. The measured grain sizes of the consolidated Al–SiC nanocomposites are also shown in this figure. It is shown that the Zener calculated grain sizes are higher, while the predicted results from Gladman's model are in close agreement with the experimentally determined grain sizes of the nanocomposites reinforced by nanometric SiC particles. Hence, it is reveal that initial grain size distribution of mechanically milled metallic nanocomposites is considerable in grain growth behavior.

The hardening mechanisms of metals and alloys, promoted by deformation, grain refinement and solid dispersion are well known. The outstanding hardness results of the Al–SiC nanocomposites samples, as shown in Fig. 10, can be related to several factors: (i) homogeneous distribution of hard nanometric SiC particles in the aluminum matrix. The particles which have high surface to volume ratio result in less mean dislocation free path and so, higher resistance to the motion of mobile dislocations. (ii) Ultra-fine structure of aluminum matrix. It is well known that a refinement of grain size leads to more grain boundaries, and then provides more ob-

stacles for dislocation pile up in the adjacent grains. Hence, it should be considered that the refinement of the aluminum grain size resulted from mechanical milling process increases the hardness of the composite according to the Hall–Petch relation. (iii) Presence of oxide particles in aluminum matrix. It should be pointed out that dispersed oxide particles in aluminum matrix induced from different sources (Table 4) could be responsible for the increased hardness in the nanocomposites.

As It was mentioned increasing the SiC nanoparticles content, due to higher degree of deformation imposed by mechanical milling process and more potential for pinning of grain boundary during consolidation process, result in lower grain size of aluminum matrix structure (Table 3). Moreover, presence of the higher hard and abrasive SiC particles content probably result in increasing the dispersed oxide particles in aluminum matrix imposed from abrasion of the alumina balls during milling. Hence, it is observed that there is a significant improvement in hardness with increasing SiC nanoparticles content. Here, it is worth to notice that due to higher degree of deformation imposed by mechanical milling process and higher applied pressure in consolidation of the aluminum powders reinforced by higher SiC nanoparticles content, the density of dislocations generated in aluminium structure increase. It could be enhance the hardness of the samples. Although, in the studied Al–SiC system, the consolidated compacts were annealed and cooled to ambient temperature at a slow rate. Therefore, this factor has no noticeable effect on increasing the hardness.



## 5. Conclusion

In the present work, processing of Al–SiC nanocomposites by high-energy mechanical milling and subsequent a double pressing/sintering route was studied. The effect of volume fraction of reinforcement particles on the milling and consolidation process was evaluated. The findings can be summarized as followings:

- The double pressing/sintering route, depending on the SiC content, is successful route to obtain high density Al-SiC nanocomposite samples without using a hot-working step.
- The grain size of the aluminum matrix in the composite powders and bulk samples decrease with higher volume fraction of SiC. This effect is more noticeable in consolidated samples due to the role of particle in pinning the grain boundary.
- The grain size predicted from Gladman's relationship shows close agreement with the experimentally determined grain size of the Al–SiC nanocomposites.
- Homogeneous distribution of nanometric SiC particles throughout the nanostructured aluminum matrix eventuate to high harness of the Al–SiC nanocomposites.

*Acknowledgements*

The authors gratefully acknowledge the High Technology Industries Center, the Iranian Ministry of Mines and Metals and Research and Technology Office of Sharif University of Technology for financial support of the research work and the Dispersive Solids Group of Darmstadt University of Technology for some experiments. The authors would like to thank Mr A. Darbandi for his assistance in the HRSEM observations.

## References

1. J. Cintas, F. G. Cuevas, J. M. Montes and E. J. Herrera, High-strength PM aluminum by milling in ammonia gas and sintering, *Script. Mater.* **53**, 1165–1170 (2005).
2. B. Yan and G. Li, Mg alloy matrix composite reinforced with TiNi continuous fiber prepared by ball-milling/hot-pressing, *Compos. A*, 1–5 (2005).
3. S. Billard, J. P. Fondere, B. Bacroix and G. F. Dirras, Macroscopic and microscopic aspects of the deformation and fracture mechanisms of ultrafine-grained aluminum processed by hot isostatic pressing, *Acta Mater.* **54**, 411–421 (2006).
4. F. Tang, M. Hagiwara and J. M. Schoenung, Formation of coarse-grained inter-particle regions during hot isostatic pressing of nanocrystalline powder, *Script. Mater.* **53**, 619–624 (2005).
5. J. B. Fogagnolo, M. H. Robert, E. M. Ruiz-Navas and J. M. Torralba, Extrusion of mechanically milled composite powder, *J. Mater. Sci.* **37**, 4603–4607 (2002).
6. J. B. Fogagnolo, M. H. Robert and J. M. Torralba, Mechanically alloyed AlN particle-reinforced Al-6061 matrix composites: powder processing, consolidation and mechanical strength and hardness of the as-extruded materials, *Mater. Sci. Eng. A* **426**, 85–94 (2006).
7. Z. Razavi Hesabi, H. R. Hafizpour and A. Simchi, An investigation on the compressibility of aluminum/nano-alumina composite powder prepared by blending and mechanical milling, *Mater. Sci. Eng. A* **454–455**, 89–98 (2007).
8. M. W. Weiser and L. C. De Jonghe, Inclusion size and sintering of composite powders, *J. Ameri. Ceram. Soc.* **71**, 125–127 (1988).
9. G. K. Williamson and W. H. Hall, X-ray line broadening from filed aluminum and wolfram, *Acta Metall.* **1**, 22–31 (1953).
10. J. B. Fogagnolo, F. Velasco, M. H. Robert and J. M. Torralba, Effect of mechanical alloying on the morphology, microstructure and properties of aluminum matrix composite powders, *Mater. Sci. Eng. A* **342**, 131–143 (2003).
11. A. L. Ortiz and L. Shaw, X-ray diffraction analysis of a severely plastically deformed aluminum alloy, *Acta Mater.* **52**, 2185–2197 (2004).
12. M. H. Maneshian, A. Simchi and Z. Razavi Hesabi, Structural changes during synthesizing of nanostructured W–20 wt% Cu composite powder by mechanical alloying, *Mater. Sci. Eng. A* **445–446**, 86–93 (2007).
13. R. Panelli and F. Ambrozio Filho, A study of a new phenomenological compacting equation, *Pow. Tech.* **114**, 255–261 (2001).
14. J. B. Fogagnolo, E. M. Ruiz-Navas, M. H. Robert and J. M. Torralba, The effects of mechanical alloying on the compressibility of aluminum matrix composite powder, *Mater. Sci. Eng. A* **355**, 50–55 (2003).
15. J. A. Rodriguez, J. M. Gallardo and E. H. Herra, An alternative route to the consolidation of mechenically alloyed aluminum powder, *Mater. Trans. JIM* **36**, 312–316 (1995).

16. J. A. Rodriguez, J. M. Gallardo and E. J. Herrera, Consolidation of mechanically alloyed aluminum by double cold-pressing and sintering, *J. Mater. Proc. Tech.* **56**, 254–262 (1996).
17. A. H. Tavakoli, A. Simchi and S. M. Seyed Reihani, Study of the compaction behavior of composite powders under monotonic and cyclic loading, *Compos. Sci. Tech.* **65**, 2094–2104 (2005).
18. S. Kamrani, A. Simchi, R. Reidel and S. M. Seyed Reihani, Effect of reinforcement volume fraction on the mechanical alloying of Al–SiC nanocomposite powders, *Pow. Metal.* **50**, 276–282 (2007).
19. C. D. Turner and M. F. Ashby, The cold isostatic pressing of composite powders — I. Experimental investigations using model powders, *Acta Mater.* **44**, 4521–4530 (1996).
20. A. R. Poster, Factors affecting the compaction of tungsten powders, *Pow. Metal.* **9**, 301–315 (1962).
21. J. Durisin, K. Durisinova, M. Orolınova and K. Saksl, Effect of the MgO particles on the nanocrystalline copper grain stability, *Mater. Lett.* **58**, 3796–3801 (2004).
22. M. Kubota and B. P. Wynne, Electron backscattering diffraction analysis of mechanically milled and spark plasma sintered pure aluminum, *Scrip. Mater.* **57**, 719–722 (2007).
23. C. Smith, Grains, phases, and interactions: an interpretation of microstructure, *Trans. Metall. Soc. AIME* **175**, 15–51 (1948).
24. P. A. Manohar, M. Ferry and T. Chandra, Five decades of the Zener equation, *ISIJ International* **38**, 913–924 (1998).
25. T. Gladman, The effect of second phase particles on grain growth, *Proc. R. Soc. London A* **294**, 298–309 (1966).
26. T. Yamasaki, Y. J. Zheng, Y. Ogino, M. Terasawa, T. Mitamura and T. Fukami, Formation of metal-TiN-TiC nanocomposite powders by mechanical alloying and their consolidation, *Mater. Sci. Eng. A* **350**, 168–172 (2003).